Rules that govern UPF1 binding to mRNA 3′ UTRs

Tatsuaki Kurosaki and Lynne E. Maquat[1]

Department of Biochemistry and Biophysics, School of Medicine and Dentistry, and Center for RNA Biology, University of Rochester, Rochester, NY 14642

Edited by James L. Manley, Columbia University, New York, NY, and approved January 18, 2013 (received for review November 14, 2012)

Nonsense-mediated mRNA decay (NMD), which degrades transcripts harboring a premature termination codon (PTC), depends on the helicase up-frameshift 1 (UPF1). However, mRNAs that are not NMD targets also bind UPF1. What governs the timing, position, and function of UPF1 binding to mRNAs remains unclear. We provide evidence that (*i*) multiple UPF1 molecules accumulate on the 3′-untranslated region (3′ UTR) of PTC-containing mRNAs and to an extent that is greater per unit 3′ UTR length if the mRNA is an NMD target; (*ii*) UPF1 binding begins ≥35 nt downstream of the PTC; (*iii*) enhanced UPF1 binding to the 3′ UTR of PTC-containing mRNA relative to its PTC-free counterpart depends on translation; and (*iv*) the presence of a 3′ UTR exon–junction complex (EJC) further enhances UPF1 binding and/or affinity. Our data suggest that NMD involves UPF1 binding along a 3′ UTR whether the 3′ UTR contains an EJC. This binding explains how mRNAs without a 3′ UTR EJC but with an abnormally long 3′ UTR can be NMD targets, albeit not as efficiently as their counterparts that contain a 3′ UTR EJC.

messenger ribonucleoprotein structure | RNA-binding protein | messenger RNA quality control

In mammalian cells, mRNAs and the pre-mRNAs from which they derive continually lose and acquire proteins in ways that reflect past and current metabolic states and influence future metabolic steps. For example, newly synthesized mRNAs, which support the pioneer round of translation, are bound by the cap-binding protein (CBP) heterodimer CBP80–CBP20 and, provided they underwent splicing, exon–junction complexes (EJCs) (1). In contrast, the bulk of cellular mRNAs have lost CBP80–CBP20 and EJCs, have acquired eukaryotic translation initiation factor (eIF)4E in the place of CBP80–CBP20, and support most of cellular translation. CBP80 and EJCs are important for nonsense-mediated mRNA decay (NMD), which down-regulates mRNAs that harbor either an exon-exon junction downstream of a termination codon (2, 3) and/or an abnormally long 3′ UTR (3–6). Thus, NMD targets newly synthesized mRNAs during the pioneer round of translation, whereas eIF4E-bound mRNAs appear to be immune to NMD (1, 3). This conclusion is supported by single-RNA fluorescent in situ-hybridization measurements of premature termination codon (PTC)-containing mRNAs in intact cells after the induction of mRNA synthesis (7).

Messenger ribonucleoprotein (mRNP) remodeling also takes place during NMD. When translation terminates at a PTC and an EJC is situated sufficiently downstream of the PTC so as not to be displaced by the terminating ribosome (8, 9), a complex called suppressor with morphogenic effect on genitalia (SMG) 1–up-frameshift 1 (UPF1)–eukaryotic release factor (eRF) 1–eRF3 (SURF) is thought to form at the PTC and, together with the downstream EJC, constitutes a decay-inducing complex (DECID) (10, 11). The transient and/or weak interaction of mRNA cap-bound CBP80 with UPF1, which occurs on mRNAs even if they are not NMD targets, promotes UPF1 binding to eRF1–eRF3 and, subsequently, to an EJC (12). Although SMG8 and SMG9 tightly associate with SMG1 to suppress its kinase activity (11, 13), the EJC constituents UPF2 and UPF3 or UPF3X (also called UPF3a or UPF3b, respectively) augment the SMG1-mediated phosphorylation of UPF1 (10). Hyperphosphorylated UPF1 then binds to eIF3 of a 43S preinitiation complex, positioned at the translation initiation codon of the NMD target, to suppress further translation initiation events (14) and promote mRNA decay (15–18). One or a combination of SMG5, SMG6, and SMG7 recruits protein phosphatase 2A to return UPF1 to its steady-state hypophosphorylated status (19–22).

The importance of NMD in human pathologies is underscored by the many genetically inherited diseases (23–25) that are due to a PTC-containing mRNA. Read-through therapies have shown promise in generating full-length proteins without concomitantly stabilizing PTC-bearing mRNAs (26, 27). However, a deeper understanding of how such transcripts are recognized and selectively degraded by NMD is needed considering that UPF1 has been reported to bind to many mammalian mRNAs regardless of PTC status (12, 28).

Here, we follow up our finding that human UPF1 binds an order of magnitude more efficiently to a PTC-containing mRNA than to its PTC-free counterpart (12) with the goal of defining rules that would predict the extent and position of UPF1 binding to mammalian-cell mRNAs. Although NMD requires translation, the translational dependence of UPF1 binding to mRNA 3′ UTRs remains controversial (28, 29). We show that UPF1 binding to PTC-containing mRNAs increases linearly as the 3′ UTR length increases. This increase is most efficient for NMD targets that bear not only a PTC but also a 3′ UTR EJC. In contrast, the increase in UPF1 binding is less dramatic for PTC-containing mRNAs that are not NMD targets. Thus, we propose that a 3′ UTR EJC changes the affinity of UPF1 for the mRNP and/or increases the number of bound UPF1. We provide evidence that the enhanced UPF1 binding to the 3′ UTR of an NMD target relative to its PTC-free counterpart depends on translation and begins ≥35 nt downstream of the PTC. UPF1 also binds to the 3′ UTRs of mRNAs that terminate translation at or downstream of the normal position, but to a much lesser extent and in a way that does not reflect 3′ UTR length. Our results lend insight into mRNP structure and function.

Results

Termination-Codon Context Determines the Extent of UPF1 Binding per Unit 3′ UTR Length. We aimed to identify which elements within NMD targets, in addition to a PTC, are important to sustain enhanced UPF1 binding. Thus, we quantitated the amount of UPF1 binding to derivatives of the same mRNA that are or are not NMD targets. In one set of experiments, the derivatives have different 3′ UTR lengths either with or without a 3′ UTR EJC so we could determine whether UPF1 binds 3′ UTRs comparably per unit length and whether a 3′ UTR EJC contributes to UPF1 binding. In another set of experiments, the derivatives have the identical 3′ UTR but do or do not harbor a 3′ UTR EJC. The second set of constructs controls for any variations in UPF1 binding that are due to variations in 3′ UTR sequence, rigorously allowing us to determine whether a 3′ UTR EJC contributes to UPF1 binding.

Initially, pdRLUC-Gl Norm, which produces mRNA that terminates translation at position 147, and PTC-containing 7Ter,

Author contributions: T.K. and L.E.M. designed research; T.K. performed research; T.K. and L.E.M. contributed new reagents/analytic tools; T.K. and L.E.M. analyzed data; and T.K. and L.E.M. wrote the paper.

The authors declare no conflict of interest.

This article is a PNAS Direct Submission.

[1]To whom correspondence should be addressed. E-mail: lynne_maquat@urmc.rochester.edu.

This article contains supporting information online at www.pnas.org/lookup/suppl/doi:10.1073/pnas.1219908110/-/DCSupplemental.

26Ter, 39Ter, 65Ter, 82Ter, 101Ter, 120Ter, and 131Ter variants of pdRLUC-Gl Norm were generated [Fig. 1*A*, where "d" specifies a deletion within the renilla luciferase (RLUC) reading frame that is in frame with the β-globin (Gl) reading frame]. PTCs 7Ter, 26Ter, 39Ter, 65Ter, and 82Ter have been shown or are expected to efficiently trigger NMD; in contrast, 101Ter, 120Ter, or 131Ter have been shown or are expected not to trigger NMD because translating ribosomes remove all EJCs (4). Additionally, pdRLUC-Gl constructs harboring 155Ter, 163Ter, or 171Ter *in cis* to a CAA Gln codon at the position of Norm Ter were generated (Fig. 1*A*). Each pdRLUC-Gl test plasmid was transiently introduced into human embryonic kidney (HEK)293T cells together with the MYC-UPF1 expression vector pCMV-MYC-UPF1 (14) or, as a control, pCMV-MYC (14), and the phCMV-MUP reference plasmid, which produces mRNA that encodes the mouse major urinary protein (MUP). The resulting cell lysates were analyzed before or after immunoprecipitation (IP) by using anti-MYC.

In this and all subsequent experiments, we achieved comparable MYC-UPF1 expression (<twofold the level of cellular UPF1) and comparable IP efficiencies for each experimental sample (Fig. 1*B*). RT-PCR revealed that before IP the level of dRLUC-Gl mRNA that harbors 7Ter, 26Ter, 39Ter, 65Ter, or 82Ter was ∼19% (i.e., 14–28%) the level of dRLUC-Gl Norm mRNA because each is subject to NMD, whereas the level of dRLUC-Gl mRNA that harbors 101Ter, 120Ter, 131Ter 155 Ter, 163Ter, or 171 Ter was ∼94% (i.e., 86–107%) the level of dRLUC-Gl Norm mRNA because each is not an NMD target (Fig. 1*C* and Table S1). After IP, the mRNAs were divided into one of three categories based on the amount of mRNA recovered: PTC-containing mRNAs that are NMD targets > PTC-containing mRNAs that are not NMD targets >> mRNAs that lack a PTC (Fig. 1 *C* and *D*). Remarkably, two key differences in UPF1 binding to PTC-containing mRNAs that are NMD targets compared with those that are not NMD targets derived from the presence of a 3′ UTR EJC. First, the change in mRNA recovery after anti-MYC IP (i.e., MYC-UPF1 binding) per unit 3′ UTR length was greater for PTC-containing mRNAs that are NMD targets compared with those that are not (Fig. 1*D*): PTC-containing mRNAs that are NMD targets had a slope of ∼3.6 (r^2 = 0.85 ± 0.12 based on three independent experiments), whereas PTC-containing mRNAs that are not NMD targets had a slope of ∼2.4 (r^2 = 0.97 ± 0.01). Second, the presence of a 3′ UTR EJC, which typified NMD targets, significantly augmented the level of mRNA recovery on top of the amount of recovery that was attributable to UPF1 binding per unit 3′ UTR length (Fig. 1*D*; see also below). mRNA recovery was least efficient for mRNAs that terminated at or downstream of the normal termination codon, and the amount of mRNA recovered did not significantly correlate with 3′ UTR length.

In controls for IP specificity, dRLUC-Gl mRNA Norm failed to coimmunoprecipitate with MYC alone (Fig. 1*C*). Furthermore, the results of lysate-mixing experiments demonstrated that the co-IP of MYC-UPF1 and dRLUC-Gl mRNA is the consequence of a bona fide cellular interaction (Fig. S1*A*). UPF1 binding to the 3′ UTRs of PTC-containing mRNAs whether the mRNA is an NMD target is specific and, data indicate, depends on translation. As one piece of evidence (see below for others), UPF1 binding to dRLUC-Gl Norm pre-mRNA was only weakly apparent (∼40-fold less than to dRLUC-Gl Norm mRNA) and did not vary depending on the position of the termination codon (Fig. S1*B*). As additional evidence, when ribosome elongation was inhibited by using puromycin, the co-IP of PTC-containing mRNAs that are and are not NMD targets with MYC-UPF1 was reduced (Fig. S1 *C*–*E*).

Importantly, when normalized to 3′ UTR length, the largest difference in UPF1 binding to PTC-containing mRNAs that are NMD targets compared with those that are not appears to be attributable the 3′ UTR EJC (Fig. 1 *C* and *D*). HEK293T cells

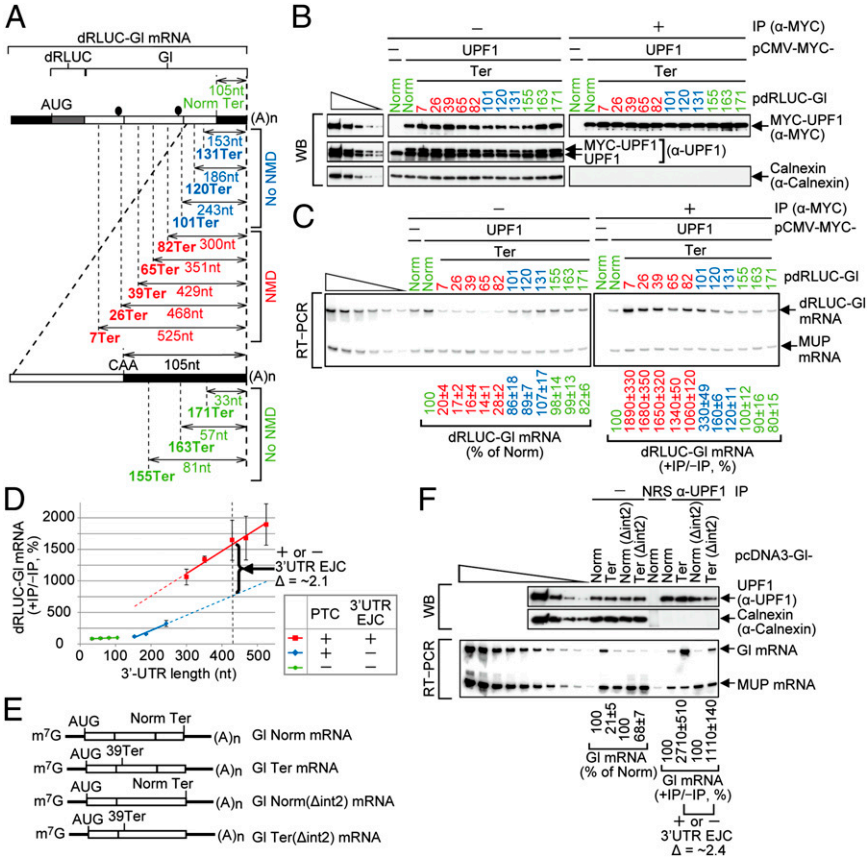

Fig. 1. Efficiency of UPF1 binding to mRNAs depends on 3′ UTR length and a 3′ UTR EJC. (*A*) Structure of dRLUC-Gl mRNA showing positions of the normal termination codon (Norm Ter), PTCs within the β-globin (Gl) translational reading frame (white boxes), or termination codons within the Gl 3′ UTR. The distance of each Ter relative to the poly(A) tail is shown in nucleotides below the corresponding double arrowheaded horizontal line. Black boxes represent UTRs, the gray box specifies 69-nt of the (d)RLUC coding region, (A)n denotes the poly(A) tail, and the two black ovals represent EJCs. (*B*) HEK293T cells (8×10^7) were transiently transfected with the specified pdRLUC-Gl test plasmid (1 μg), the phCMV-MUP reference plasmid (0.5 μg), and pCMV-MYC-UPF1 (1 μg) or, as a control, pCMV-MYC (1 μg). Cell lysates were immunoprecipitated by using anti(α)-MYC and analyzed before (–) or after (+) IP by Western blotting (WB). (*C*) RT-PCR of samples from *B*, where before or after IP the level of dRLUC-Gl mRNA was normalized to the level of MUP mRNA, and the normalized level of dRLUC-Gl Norm mRNA was defined as 100%. The normalized level after IP was then calculated as a ratio of the normalized level before IP, where the ratio for dRLUC-Gl Norm mRNA was defined as 100%. (*D*) Plot of the amount of UPF1 binding to each dRLUC-Gl mRNA from *C* relative to 3′ UTR length. The bracket shows the change in amount (Δ) of dRLUC-Gl 39Ter mRNA that coimmunoprecipitated with UPF1 that is attributable to its 3′ UTR EJC(s). (*E*) Diagrams of Gl Norm or Ter mRNAs with or without (Δ) intron 2. (*F*) Transfections, IPs and analyses were as in *B* and *C*, except the specified pcDNA-Gl plasmid was used in place of a pdRLUC-Gl plasmid. Quantitations derive from at least three independently performed experiments and represent the mean ± SDs.

expressing Gl 39Ter mRNA coimmunoprecipitated with ~2.4-fold more UPF1 than did Gl 39Ter mRNA produced from the same gene that (*i*) lacks intron 2 (Δint2), (*ii*) has the identical 3′ UTR length, and (*iii*) is targeted for NMD, albeit inefficiently, because of its abnormally long 3′ UTR (Fig. 1 *E* and *F*). This ~2.4-fold increase is comparable to the ~2.1-fold increase in the co-IP of UPF1 with dRLUC-Gl 39Ter mRNA that appears to be due to a 3′ UTR EJC (Fig. 1*D*; see bracket, which shows the differential between the solid-red line and dotted-blue line for dRLUC-Gl 39Ter mRNA). As expected given the positive role of the 3′-most intron in RNA 3′-end formation (30), the absence of intron 2 in either Gl Norm or Gl Ter mRNA decreased the level of mRNA before IP (Fig. 1*F*). Also as expected, the amount of UPF1 binding to Gl Norm or Gl Norm (Δint2) mRNA (when normalized to the level of mRNA before IP) was comparable (Fig. 1*F*).

Enhanced UPF1 Binding to PTC-Containing Gl mRNA Compared with Its PTC-Free Counterpart Depends on Translation. Translation initiation and elongation inhibitors are known to block NMD, but UPF1 binding to mRNA 3′ UTRs has been reported to occur independently of ongoing translation (28). To further investigate the influence of translation on UPF1 binding, we compared HeLa cells that stably express either IRE-Gl Ter mRNA or IRE-Gl Norm mRNA, each of which contains in its 5′ UTR the iron-responsive element (IRE) from the 5′ UTR of ferritin heavy-chain mRNA (Fig. 2*A*) (9, 31). Cells were cultured for 1 d in Dulbecco's modified Eagle's medium (DMEM) containing 10% fetal bovine serum (FBS) after which the iron-chelator deferoxamine mesylate (Df) was added to repress IRE-Gl mRNA translation. After 24 h, cells were washed and subsequently cultured in fresh DMEM containing 10% serum and either Df or hemin, which is a porphyrin that supplies iron and thereby promotes IRE-Gl mRNA translation, for 0, 1, 3, 6, 8, 12, or 24 h before lysis. Upon the addition of fresh medium, the promoter that drives IRE-Gl gene expression provided a burst in pre-mRNA synthesis that returned to steady state by 8 h (Fig. S2 *A* and *B*). Protein and RNA in cell lysates before or after IP using either anti-UPF1 or, as a control for nonspecific IP, normal rabbit serum (NRS) were analyzed by Western blotting and RT-PCR, respectively.

As expected, ferritin, which provides a measure of IRE function, was essentially undetectable in cells exposed for 24 h to Df (Fig. 2*B* and Fig. S2*C*) but was abundant in cells exposed for 24 h to hemin (Fig. 2*B* and Fig. S2*D*). Also as expected, RT-PCR of RNA before IP revealed that hemin (and the resulting translation) promoted IRE-Gl NMD so that the level of IRE-Gl Ter mRNA was reduced to ~23% the level of IRE-Gl Norm mRNA, whereas Df inhibited IRE-Gl NMD (and translation) so that the level of IRE-Gl Ter mRNA was ~80% the level of IRE-Gl Norm mRNA (Fig. 2*B*).

Consistent with an induction of IRE-Gl Norm gene expression when cells were transferred to fresh DMEM supplemented with 10% serum at 0 h followed by a return to steady state by 8 h, the level of IRE-Gl Norm mRNA increased during the first 6 h after serum addition and did not decrease thereafter regardless of its translational status (Fig. 2*C* and Fig. S2*E*), which undoubtedly reflects the >24-h half-life of β-Gl mRNA in nonerythroid cells (32). Although the level of IRE-Gl Ter mRNA likewise increased during the first 6 h after the addition of fresh medium regardless of the presence of Df or hemin, a sharp drop was observed after the 6-h time point in the presence of hemin but not in the presence of Df (Fig. 2*D* and Fig. S2*F*). In support of this drop being attributable to NMD, the drop coincided with the translational activation of ferritin mRNA (Fig. S2*D*) and, thus, the translational activation of IRE-Gl mRNA. Furthermore, the drop coincided with the accumulation of a reported 3′-degradation product of Gl Ter mRNA (18) that was evident by using cells in which the 5′-to-3′ exonuclease XRN1 was down-regulated (Fig. S2 *G*–*I*): Down-regulating XRN1 in mammalian cells has been shown to result in the accumulation of a SMG6

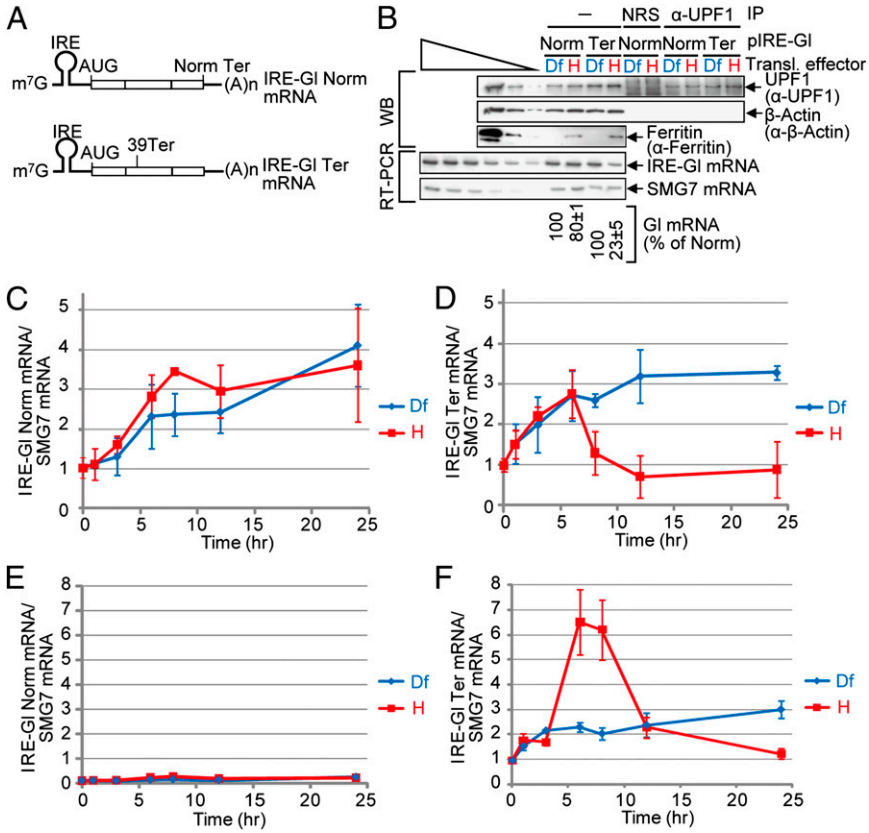

Fig. 2. Enhanced UPF1 binding to PTC-containing Gl mRNA compared with its PTC-free counterpart depends on translation. (*A*) Diagram of IRE-Gl Ter mRNA, where the 5′ cap, 35-nt iron-responsive element of ferritin heavy-chain mRNA, initiation codon, PTC, normal termination codon, and poly(A) tail are represented, respectively, by m^7G, IRE, AUG, 39Ter, Norm Ter, and (A)n. Horizontal lines represent the β-globin (Gl) 5′ UTR or 3′ UTR; boxes represent coding regions. (*B*) HeLa cells (1×10^7) stably expressing either IRE-Gl Norm mRNA or IRE-Gl Ter mRNA were cultured in 100 μM deferoxamine mesylate (Df) and subsequently in 100 μM of either Df, which inhibits IRE-Gl and ferritin mRNA translation, or hemin (H), which promotes IRE-Gl and ferritin mRNA translation, for 24 h. Western blotting and RT-PCR were performed before (–) or after anti (α)-UPF1 IP or, to control for nonspecific IP, normal rabbit serum (NRS). For samples before IP, the level of IRE-Gl mRNA was normalized to the level of SMG7 mRNA, and the normalized level of IRE-Gl Norm mRNA in the presence of Df was defined as 100%. (*C*) Plot of RT-PCR data of IRE-Gl Norm mRNA obtained at 0, 1, 3, 6, 8, 12, and 24 h after the addition of either Df or hemin. The level of IRE-Gl Norm mRNA was normalized to the level of SMG7 mRNA and defined as 1 at time 0. (*D*) As in *C* except cells expressing IRE-Gl Ter mRNA were analyzed. (*E*) As in *C*, except cells were analyzed after anti-UPF1 IP, and the level of immunoprecipitated IRE-Gl Norm mRNA was normalized to the level of immunoprecipitated SMG7 mRNA. (*F*) As in *D*, except cells were analyzed after anti-UPF1 IP, and the level of immunoprecipitated IRE-Gl Ter mRNA was normalized to the level of immunoprecipitated SMG7 mRNA. Quantitations derive from three independently performed experiments and represent the mean ± SDs.

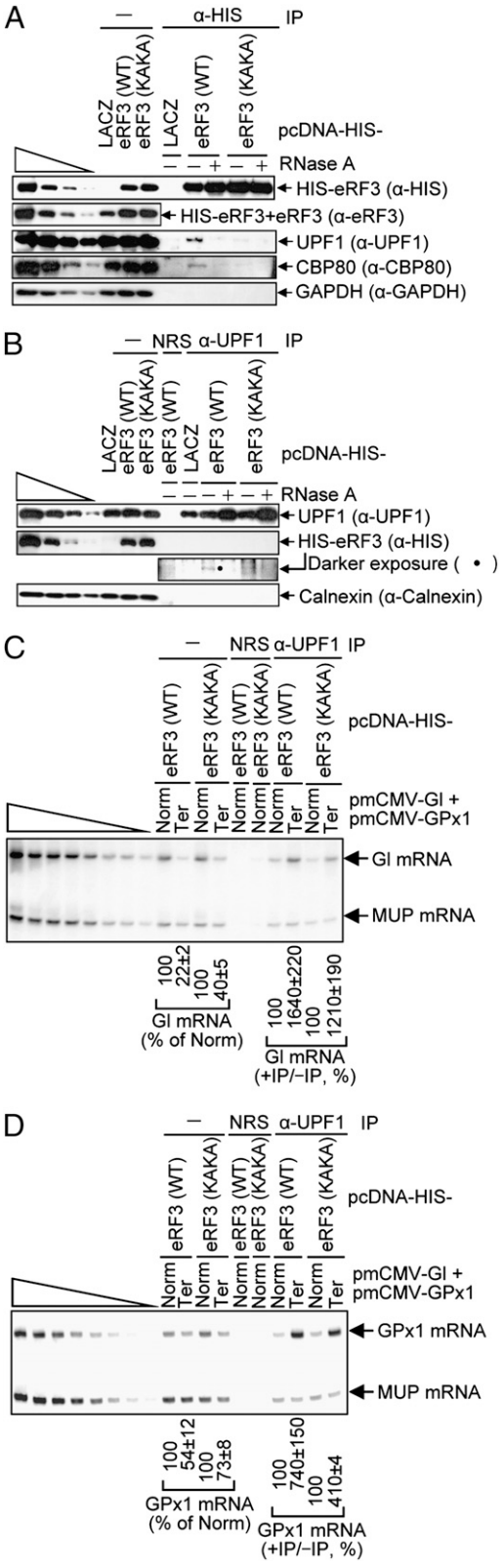

Fig. 3. Evidence that eRF3 influences UPF1 binding to PTC-containing mRNA. (*A*) HEK293T cells (8×10^7) were transiently transfected with 9 μg of pcDNA-HIS-eRF3(WT), pcDNA-HIS-eRF3(KAKA) or, as a control, pcDNA-HIS-LACZ. Cells were analyzed by Western blotting before (–) or after IP in the absence or presence of RNase A by using anti(α)-HIS. (*B*) HEK293T cells (8×10^7) were transiently transfected with (*i*) pmCMV-Gl Norm (1 μg), pmCMVGPx1 Ter (1 μg), and phCMV-MUP (0.5 μg) or pmCMV-Gl Ter (1 μg), pmCMVGPx1 Norm (1 μg), and phCMV-MUP (0.5 μg) and (*ii*) 9 μg of pcDNA-HIS-eRF3(WT), pcDNA-HIS-eRF3(KAKA), or pcDNA-HIS-LACZ. IPs were performed in the presence of RNase A by using anti-UPF1 or, to control for nonspecific IP, normal rabbit serum (NRS). (*C* and *D*) RT-PCR analyses essentially as in Fig. 1. Quantitations derive from three independently performed experiments and represent the mean ± SDs.

endonuclease-generated 3′-cleavage product of PTC-containing mRNA (16–18).

IP using anti-UPF1 demonstrated that the level of UPF1 binding to IRE-Gl Norm mRNA was just above background throughout the time course regardless of IRE-Gl Norm mRNA translational status (Fig. 2*E* and Fig. S2*J*). This level was ∼10–20-fold higher for IRE-Gl Ter mRNA (Fig. 2 *E* and *F*) possibly because IRE-Gl Ter mRNA contains a larger 3′ UTR, which allows for more nonspecific UPF1 binding (28). Nevertheless, UPF1 binding to IRE-Gl Ter mRNA in the presence of translation peaked at 6–8 h at a level that was ∼26-fold above the level of UPF1 binding to IRE-Gl Norm mRNA (Fig. 2*F* and Fig. S2*K*).

We conclude that enhanced binding of UPF1 to PTC-containing mRNA precedes mRNA decay (Fig. 2*D* and Fig. S2 *G–I*), indicating that bound UPF1 is poised to contribute to the decay process. This enhanced binding at 6–8 h of hemin treatment requires translation as was evident by its absence when IRE-Gl Ter mRNA was not translated (Fig. 2*F* and Fig. S2*K*).

eRF3 Function Influences UPF1 Binding to PTC-Containing mRNA. To begin to define when the process of translation-enhanced UPF1 binding to an NMD target occurs, it made sense to focus on the last step of translation given that translation termination defines the 3′ UTR. We focused on the requirement for eRF3 because it interacts directly with UPF1 during translation termination (6, 33, 34). To this end, HEK293T cells were transiently transfected with pcDNA-HIS-eRF3(WT) or pcDNA-HIS-eRF3(KAKA), which produce respectively histidine(HIS)-tagged wild-type (WT) eRF3 or HIS-tagged eRF3 harboring L69K, N72A, A73K, and F76A (KAKA) (6) or, as a control, pcDNA-HIS-LACZ, which produces mRNA that encodes HIS-tagged *E. coli* β-galactosidase mRNA. HIS-eRF3 (KAKA) fails to bind not only UPF1, thereby failing to support SURF complex formation, but also the largely cytoplasmic poly(A)-binding protein PABPC1 (6). Western blotting before IP or after IP in the presence of RNase A, which degraded cellular RNA, demonstrated that HIS-eRF3(WT) and HIS-eRF3(KAKA) were expressed at a comparable level that was only ∼1.3-fold above the level of endogenous eRF3 (Fig. 3*A*). As expected, the co-IP of HIS-eRF3(KAKA) with UPF1 and, as a consequence, CBP80 was only ∼15% that of HIS-eRF3(WT), consistent with SURF-complex formation on CBP80-bound mRNA during the process of translation termination (Fig. 3*A*). The finding that the co-IP of HIS-eRF3(WT) with UPF1 was RNase A sensitive (Fig. 3*A*) although UPF1 binding directly to eRF3 (6, 33, 34) indicates that most of UPF1 binding is not to eRF3 but, presumably, to 3′ UTRs and their EJCs. We do not think that UPF1 binding is mediated by eRF3 binding to poly(A)-bound PABPC1 because data indicate a complex of UPF1–eRF3–PABPC1 cannot be detected by using purified proteins (6).

The transfections with pcDNA-HIS-eRF3(WT) or pcDNA-HIS-eRF3(KAKA) were repeated to include a mixture of either (*i*) pmCMV-Gl Norm, pmCMV-GPx1 Ter (where GPx1 denotes glutathione peroxidase 1), and phCMV-MUP or (*ii*) pmCMV-Gl Ter, pmCMV-GPx1 Norm, and phCMV-MUP, and IPs were performed by using anti-UPF1 or, as a control, NRS. The co-IP of HIS-eRF3(KAKA) with UPF1 was undetectable (Fig. 3*B*). Using samples that were not treated with RNase A, HIS-eRF3(KAKA) not only decreased the efficiency of Gl Ter or GPx1 Ter NMD ∼1.8-fold or ∼1.4-fold, respectively, but also decreased the extent of UPF1 binding to Gl Ter mRNA or GPx1 Ter mRNA ∼1.4-fold and ∼1.8-fold, respectively (Fig. 3 *C* and *D*). Although the changes observed by expressing eRF3(KAKA) were modest, most likely

due to the presence of a comparable level of cellular eRF3, data obtained suggest that UPF1 binding to eRF3 during recognition of a PTC (i.e., during translation termination) enhances UPF1 binding to substrate mRNAs and to 3′ UTR EJCs. Thus, these findings, like our previous findings (Fig. 2), indicate that ongoing translation is required for the enhanced binding of UPF1 the 3′ UTRs of PTC-containing mRNAs compared with their PTC-free counterparts.

UPF1 Binding to 3′ UTRs Begins ≥35-Nt Downstream of a PTC. With the finding that translation termination is central to the mechanism by which UPF1 discriminates between mRNAs that are and are not NMD targets, we next asked at what position(s) UPF1 binds to its substrate mRNAs. HeLa cells that stably express IRE-Gl Ter mRNA were cultured as described above for the 8-h exposure to Df or hemin. Lysates from cells cultured in the presence of hemin were subsequently immunoprecipitated by using anti-UPF1 or, as a control, NRS. After extensive washing, UPF1-bound RNAs were incubated with RNase H in the absence or presence of one of four antisense DNA oligonucleotides (Fig. 4*A*) while the RNAs were associated with antibody–protein A agarose beads. By so doing, cleavage products (CPs) that do not associate with UPF1 can be distinguished from those that do. Although this approach will not demonstrate that longer 3′ UTRs associate more efficiently with UPF1 as was shown in Fig. 1, it has two important advantages over cleaving before IP: it obviates RNA decay that could occur after cleavage during the IP, and all UPF1-bound samples will manifest the same IP efficiency. IRE-Gl Ter mRNA 5′-CPs consisted of 185, 241, 320, or 434 nt and contained, respectively, 0, 35, 114, or 228 nt of 3′ UTR (where 3′ UTR nt 1 is defined as the nt immediately downstream of Ter) (Fig. 4*B*). The corresponding 3′-CPs consisted of 439, 383, 303, or 190 nt, all of which derive from the 3′ UTR except for the Oligo 1 3′-CP, which contains 5 nt of coding region plus Ter (Fig. 4*B*). Notably, the 434-nt 5′-CP and the 439-, 383-, and 303-nt 3′-CPs contain the 3′ UTR EJC.

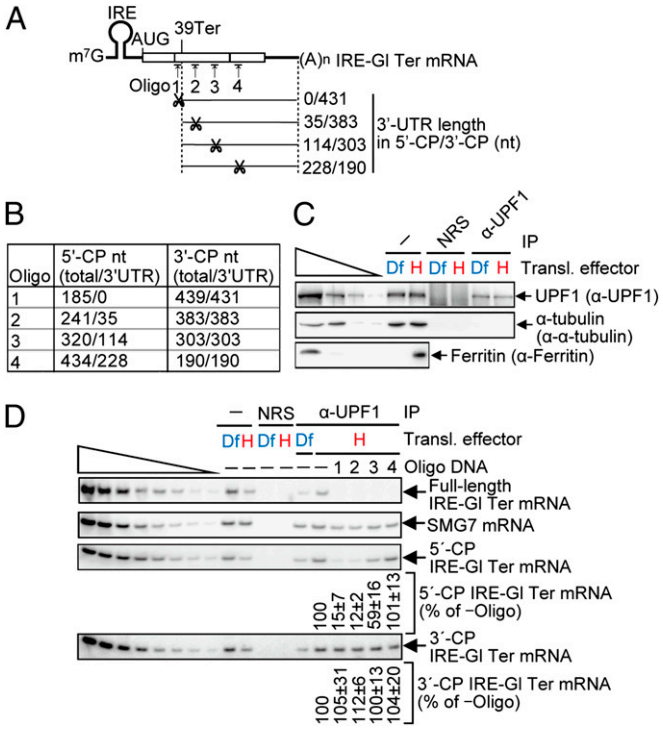

Oligo	5′-CP nt (total/3′UTR)	3′-CP nt (total/3′UTR)
1	185/0	439/431
2	241/35	383/383
3	320/114	303/303
4	434/228	190/190

Fig. 4. UPF1 binding to Gl Ter 3′ UTRs begins ≥35-nt downstream of the PTC. (*A*) Essentially as in Fig. 2*A*, except that only IRE-Gl Ter mRNA is shown, the scissors indicate a site of oligonucleotide DNA (oligo)-directed RNase H cleavage, and the numbers to the right of the scissors specify the number of 3′ UTR nucleotides in the resulting 5′- and 3′-cleavage products (CPs). (*B*) Table of the number of total nt/3′ UTR nt in the 5′-CPs and 3′-CPs that result from the RNase H-mediated cleavage of IRE-Gl Ter mRNA as directed by the denoted DNA oligo. (*C*) HeLa cells stably expressing IRE-Gl Ter mRNA were cultured as in Fig. 2, except exposure to either Df or hemin (H) was for 8 h. Western blotting was performed before (–) or after anti(α)-UPF1 IP or, to control for nonspecific IP, NRS using samples that were not incubated with oligonucleotide. (*D*) RT-PCR using samples analyzed in *C* and also samples that were subjected to RNase H cleavage that was directed by the specified oligonucleotide. For samples that were cleaved in the presence of hemin, the level of each CP was normalized to the level of SMG7 mRNA, and resulting values were then normalized to the level of uncleaved IRE-Gl Ter mRNA in the presence of hemin, which was defined as 100%. Quantitations derive from two to three independently performed experiments and represent the mean ± SDs.

As expected, before IP Df (but not hemin) blocked the production of ferritin (Fig. 4*C*) and increased the level of IRE-Gl Ter mRNA before RNase H-mediated cleavage, i.e., inhibited NMD (Fig. 4*D*). Cleavage was complete as indicated by the nearly complete loss of full-length IRE-Gl Ter mRNA (Fig. 4*D*). Also as expected, relative to Df, hemin enhanced (by ∼5.8-fold) the amount of uncleaved IRE-Gl Ter mRNA that coimmunoprecipitated with UPF1 (Fig. 4*D*).

The efficiencies with which the four 3′-CPs coimmunoprecipitated with UPF1 in samples exposed to hemin were comparable to the efficiency with which UPF1 coimmunoprecipitated with uncleaved IRE-Gl Ter mRNA, suggesting that all 3′-CPs were bound by at least one UPF1 molecule (Fig. 4*D*). UPF1 binding to 5′-CPs containing either 0 or 35 nt of 3′ UTR was only ∼14% the level of binding to uncleaved IRE-Gl Ter mRNA, and UPF1 binding to 5′-CPs containing 114 or 228 nt of 3′ UTR increased to, respectively, ∼59% or ∼101% (Fig. 4*D*). We conclude that UPF1 was absent from the 5′ UTR coding region (oligo 1 data) and first 35 nt of the 3′ UTR (oligo 2 data) of translationally active IRE-Gl Ter mRNA, suggesting that UPF1 was occluded from the 5′-most 3′ UTR sequences by the terminating ribosome. UPF1 binding becomes apparent between 35 and 114 nt downstream of the termination codon (oligo 3 data) and is further enriched to exist comparably on both 5′- and 3′-CPs containing, respectively, 228 and 190 nt of 3′ UTR (oligo 4 data), indicating that at least one UPF1 molecule exists on both CPs, the latter of which consists exclusively of sequences downstream of the 3′-most EJC. Thus, we suggest that more than one UPF1 is associated with the 3′ UTR of an NMD target: UPF1 appears to be binding the full-length of the 3′ UTR after the first 35 nt.

Discussion

Based in the findings that (*i*) longer 3′ UTRs were bound by higher levels of UPF1 (Figs. 1 and 2) and (*ii*) the same level of Gl mRNP was recovered by using anti-UPF1 when assaying intact Gl mRNP or either half of Gl mRNP that was cleaved midway into the 3′ UTR (Fig. 4), we suggest that multiple UPF1 molecules bind to the 3′ UTR of PTC-containing mRNAs. UPF1 binding was observed both upstream and downstream of the 3′ UTR EJC (Fig. 4*D*). We also suggest that binding is directly to the mRNA 3′ UTR: Although the domains of eRF3 that interact with UPF1 and with PABPC1 appear to be distinct (34, 35), raising the possibility that some UPF1 binding could derive from the interaction between eRF3 and poly(A)-bound PABPC1, experiments performed by using purified proteins in vitro failed to show that the interaction between UPF1 and eRF3 coexists with the interaction between eRF3 and PABPC1 (6).

UPF1 binding is to an extent that is greater per unit 3′ UTR length if the mRNA is an NMD target, and the presence of a 3′ UTR EJC further enhances UPF1 binding and/or affinity (Fig. 1). The 3′ UTRs of mRNAs that terminate translation at or downstream of their normal termination codon bind the least amount of UPF1 in a way that does not significantly correlate with 3′ UTR length (Fig. 1).

Results described here indicate that UPF1 binds to newly synthesized PTC-containing mRNAs whether the mRNAs are NMD targets. UPF1 binds to the 3′ UTRs of PTC-containing mRNAs at

the PTC as part of the SURF complex via its interaction with eRF3, which is promoted by the interaction of UPF1 with CBP80 (12). UPF1 then loads onto the 3′ UTRs of mRNAs beginning ≥35 nt downstream of the PTC (Fig. 4), which undoubtedly reflects space occupied on the 3′ UTR by the terminating ribosome. The recent report that a hairpin inserted downstream of a termination codon accumulates UPF1 (29) supports the idea that UPF1 translocates along the 3′ UTR. Data indicate that translocation occurs after translation termination at a PTC (Fig. 3). Should there exist a 3′ UTR EJC that is not removed by the terminating ribosome, then the number and/or affinity of bound UPF1 increases (Fig. 1). It is this increase that distinguishes a PTC-containing mRNA that is an NMD target from one that is not. We find that UPF1 binding is indistinguishable whether there is one or two 3′ UTR EJCs (Fig. 1), most likely indicating that the so-called DECID complex (10) involves the 3′ UTR EJC that resides closest to the PTC. UPF1 binding to EJC-bound UPF2 increases UPF1 ATPase and helicase activities (36) to augment UPF1 movement along the mRNA 3′ UTR in a 5′-to-3′ direction (29), the concomitant removal of mRNP proteins from the mRNA, and mRNA decay (18).

From studies of *Saccharomyces cerevisiae*, it has been reported that the efficiency of termination-complex formation and/or translation termination varies depending on whether cells express UPF1 (37). Possibly, every termination event during the pioneer round of translation has the potential to involve UPF1. However, the degree of UPF1 loading onto a 3′ UTR and, thus, whether NMD occurs is dictated by the stability of UPF1 binding to eRF1–eRF3 at a termination codon. Loading can be further augmented by the presence of a 3′ UTR EJC.

Materials and Methods

Cell Transfections and Lysis. HeLa or HEK 293T cells were propagated in Dulbecco's modified Eagle's medium (DMEM) supplemented with 10% (vol/vol) FBS and, when specified, transiently transfected with plasmid DNA by using Lipofectamine 2000 (Invitrogen). Where indicated, HEK293T cells were cultured with 100 μg/mL puromycin (Invitrogen) for 6 h before lysis. In experiments using hemin or deferoxamine mesylate (Df), HeLa cells stably expressing either IRE-Gl Norm or IRE-Gl Ter (9) were split 1:6 and grown to a confluency of 60%, at which time Df was added to 100 μM. After an additional 24 h, cells were washed three times with phosphate-buffered saline (PBS) and subsequently cultured in DMEM plus 10% FBS containing either Df or hemin for the designated time before lysis. In all experiments, total-cell lysates were prepared by using hypotonic gentle lysis buffer (10 mM Tris at pH 7.4, 10 mM NaCl, 10 mM EDTA, and 0.5% (wt/wt) Triton X-100) (38) with protease inhibitor mixture (Roche). Protein was analyzed after the addition of NaCl to 150 mM, and RNA was extracted and purified by using TRIzol reagent (Invitrogen).

Plasmids, Immunoprecipitations, siRNA-Mediated Down-Regulation, Western Blotting, RT-PCR, and RT-qPCR. See *SI Materials and Methods*.

ACKNOWLEDGMENTS. We thank A. Geballe for pcDNA3.1-HIS-eRF3; J. Lykke-Andersen for pcDNA3-Gl Norm-MS2bs; H. Sato for pcDNA3.1-HIS-eRF3(KAKA); and M. Popp, R. Elbarbary, and D. Ermolenko for comments. This work was supported by National Institutes of Health Grant R01 GM59614 (to L.E.M.).

1. Maquat LE, Tarn WY, Isken O (2010) The pioneer round of translation: Features and functions. *Cell* 142(3):368–374.
2. Zhang J, Sun X, Qian Y, Maquat LE (1998) Intron function in the nonsense-mediated decay of beta-globin mRNA: Indications that pre-mRNA splicing in the nucleus can influence mRNA translation in the cytoplasm. *RNA* 4(7):801–815.
3. Ishigaki Y, Li X, Serin G, Maquat LE (2001) Evidence for a pioneer round of mRNA translation: mRNAs subject to nonsense-mediated decay in mammalian cells are bound by CBP80 and CBP20. *Cell* 106(5):607–617.
4. Matsuda D, Hosoda N, Kim YK, Maquat LE (2007) Failsafe nonsense-mediated mRNA decay does not detectably target eIF4E-bound mRNA. *Nat Struct Mol Biol* 14(10): 974–979.
5. Eberle AB, Stalder L, Mathys H, Orozco RZ, Mühlemann O (2008) Posttranscriptional gene regulation by spatial rearrangement of the 3′ untranslated region. *PLoS Biol* 6(4):e92.
6. Singh G, Rebbapragada I, Lykke-Andersen J (2008) A competition between stimulators and antagonists of Upf complex recruitment governs human nonsense-mediated mRNA decay. *PLoS Biol* 6(4):e111.
7. Trcek T, Sato H, Singer RH, Maquat LE (2013) Temporal and spatial characterization of nonsense-mediated mRNA decay. *Genes Dev*, in press.
8. Gehring NH, Lamprinaki S, Kulozik AE, Hentze MW (2009) Disassembly of exon junction complexes by PYM. *Cell* 137(3):536–548.
9. Sato H, Maquat LE (2009) Remodeling of the pioneer translation initiation complex involves translation and the karyopherin importin beta. *Genes Dev* 23(21):2537–2550.
10. Kashima I, et al. (2006) Binding of a novel SMG-1-Upf1-eRF1-eRF3 complex (SURF) to the exon junction complex triggers Upf1 phosphorylation and nonsense-mediated mRNA decay. *Genes Dev* 20(3):355–367.
11. Yamashita A, et al. (2009) SMG-8 and SMG-9, two novel subunits of the SMG-1 complex, regulate remodeling of the mRNA surveillance complex during nonsense-mediated mRNA decay. *Genes Dev* 23(9):1091–1105.
12. Hwang J, Sato H, Tang Y, Matsuda D, Maquat LE (2010) UPF1 association with the cap-binding protein, CBP80, promotes nonsense-mediated mRNA decay at two distinct steps. *Mol Cell* 39(3):396–409.
13. Fernández IS, et al. (2011) Characterization of SMG-9, an essential component of the nonsense-mediated mRNA decay SMG1C complex. *Nucleic Acids Res* 39(1):347–358.
14. Isken O, et al. (2008) Upf1 phosphorylation triggers translational repression during nonsense-mediated mRNA decay. *Cell* 133(2):314–327.
15. Lejeune F, Li X, Maquat LE (2003) Nonsense-mediated mRNA decay in mammalian cells involves decapping, deadenylating, and exonucleolytic activities. *Mol Cell* 12(3): 675–687.
16. Huntzinger E, Kashima I, Fauser M, Saulière J, Izaurralde E (2008) SMG6 is the catalytic endonuclease that cleaves mRNAs containing nonsense codons in metazoan. *RNA* 14(12):2609–2617.
17. Eberle AB, Lykke-Andersen S, Mühlemann O, Jensen TH (2009) SMG6 promotes endonucleolytic cleavage of nonsense mRNA in human cells. *Nat Struct Mol Biol* 16(1):49–55.
18. Franks TM, Singh G, Lykke-Andersen J (2010) Upf1 ATPase-dependent mRNP disassembly is required for completion of nonsense-mediated mRNA decay. *Cell* 143(6):938–950.
19. Chiu SY, Serin G, Ohara O, Maquat LE (2003) Characterization of human Smg5/7a: A protein with similarities to *Caenorhabditis elegans* SMG5 and SMG7 that functions in the dephosphorylation of Upf1. *RNA* 9(1):77–87.
20. Ohnishi T, et al. (2003) Phosphorylation of hUPF1 induces formation of mRNA surveillance complexes containing hSMG-5 and hSMG-7. *Mol Cell* 12(5):1187–1200.
21. Fukuhara N, et al. (2005) SMG7 is a 14-3-3-like adaptor in the nonsense-mediated mRNA decay pathway. *Mol Cell* 17(4):537–547.
22. Okada-Katsuhata Y, et al. (2012) N- and C-terminal Upf1 phosphorylations create binding platforms for SMG-6 and SMG-5:SMG-7 during NMD. *Nucleic Acids Res* 40(3):1251–1266.
23. Frischmeyer PA, Dietz HC (1999) Nonsense-mediated mRNA decay in health and disease. *Hum Mol Genet* 8(10):1893–1900.
24. Khajavi M, Inoue K, Lupski JR (2006) Nonsense-mediated mRNA decay modulates clinical outcome of genetic disease. *Eur J Hum Genet* 14(10):1074–1081.
25. Nicholson P, et al. (2010) Nonsense-mediated mRNA decay in human cells: Mechanistic insights, functions beyond quality control and the double-life of NMD factors. *Cell Mol Life Sci* 67(5):677–700.
26. Linde L, Kerem B (2008) Introducing sense into nonsense in treatments of human genetic diseases. *Trends Genet* 24(11):552–563.
27. Bhuvanagiri M, Schlitter AM, Hentze MW, Kulozik AE (2010) NMD: RNA biology meets human genetic medicine. *Biochem J* 430(3):365–377.
28. Hogg JR, Goff SP (2010) Upf1 senses 3'UTR length to potentiate mRNA decay. *Cell* 143(3):379–389.
29. Shigeoka T, Kato S, Kawaichi M, Ishida Y (2012) Evidence that the Upf1-related molecular motor scans the 3′-UTR to ensure mRNA integrity. *Nucleic Acids Res* 40(14): 6887–6897.
30. Nesic D, Maquat LE (1994) Upstream introns influence the efficiency of final intron removal and RNA 3′-end formation. *Genes Dev* 8(3):363–375.
31. Thermann R, et al. (1998) Binary specification of nonsense codons by splicing and cytoplasmic translation. *EMBO J* 17(12):3484–3494.
32. Shyu AB, Greenberg ME, Belasco JG (1989) The c-fos transcript is targeted for rapid decay by two distinct mRNA degradation pathways. *Genes Dev* 3(1):60–72.
33. Czaplinski K, et al. (1998) The surveillance complex interacts with the translation release factors to enhance termination and degrade aberrant mRNAs. *Genes Dev* 12(11):1665–1677.
34. Ivanov PV, Gehring NH, Kunz JB, Hentze MW, Kulozik AE (2008) Interactions between UPF1, eRFs, PABP and the exon junction complex suggest an integrated model for mammalian NMD pathways. *EMBO J* 27(5):736–747.
35. Kervestin S, Li C, Buckingham R, Jacobson A (2012) Testing the faux-UTR model for NMD: Analysis of Upf1p and Pab1p competition for binding to eRF3/Sup35p. *Biochimie* 94(7):1560–1571.
36. Chakrabarti S, et al. (2011) Molecular mechanisms for the RNA-dependent ATPase activity of Upf1 and its regulation by Upf2. *Mol Cell* 41(6):693–703.
37. Ghosh S, Ganesan R, Amrani N, Jacobson A (2010) Translational competence of ribosomes released from a premature termination codon is modulated by NMD factors. *RNA* 16(9):1832–1847.
38. Lykke-Andersen J, Shu MD, Steitz JA (2000) Human Upf proteins target an mRNA for nonsense-mediated decay when bound downstream of a termination codon. *Cell* 103(7):1121–1131.